

# Extracellular matrix production and calcium carbonate precipitation by coral cells *in vitro*

Yael Helman\*, Frank Natale\*, Robert M. Sherrell†, Michèle LaVigne‡, Valentin Starovoytov‡, Maxim Y. Gorbunov\*, and Paul G. Falkowski\*<sup>§¶</sup>

\*Environmental Biophysics and Molecular Ecology Program and †Inorganic Analytical Laboratory, Institute of Marine and Coastal Sciences, Rutgers, The State University of New Jersey, 71 Dudley Road, New Brunswick, NJ 08901; ‡Department of Cell Biology and Neuroscience, Rutgers, The State University of New Jersey, 604 Allison Road, Piscataway, NJ 08854; and §Department of Earth and Planetary Sciences, Rutgers, The State University of New Jersey, 610 Taylor Road, Piscataway, NJ 08854

Contributed by Paul G. Falkowski, November 8, 2007 (sent for review September 15, 2007)

The evolution of multicellularity in animals required the production of extracellular matrices that serve to spatially organize cells according to function. In corals, three matrices are involved in spatial organization: (i) an organic ECM, which facilitates cell–cell and cell–substrate adhesion; (ii) a skeletal organic matrix (SOM), which facilitates controlled deposition of a calcium carbonate skeleton; and (iii) the calcium carbonate skeleton itself, which provides the structural support for the 3D organization of coral colonies. In this report, we examine the production of these three matrices by using an *in vitro* culturing system for coral cells. In this system, which significantly facilitates studies of coral cell physiology, we demonstrate *in vitro* excretion of ECM by primary (non-dividing) tissue cultures of both soft (*Xenia elongata*) and hard (*Montipora digitata*) corals. There are structural differences between the ECM produced by *X. elongata* cell cultures and that of *M. digitata*, and ascorbic acid, a critical cofactor for proline hydroxylation, significantly increased the production of collagen in the ECM of the latter species. We further demonstrate *in vitro* production of SOM and extracellular mineralized particles in cell cultures of *M. digitata*. Inductively coupled plasma mass spectrometry analysis of Sr/Ca ratios revealed the particles to be aragonite. *De novo* calcification was confirmed by following the incorporation of <sup>45</sup>Ca into acid labile macromolecules. Our results demonstrate the ability of isolated, differentiated coral cells to undergo fundamental processes required for multicellular organization.

aragonite | cell culture | cnidaria | calcification |

Corals (class, Anthozoa) are the most basal cnidarians and the first animal phylum with an organized neural system and complex active behavior (1). The embryonic gastrula develops to form an outer ectoderm and an inner endoderm separated by the mesoglea, a noncellular fibrous jelly-like material (2). The two germ layers are spatially structured by an ECM in which embedded, interstitial (stem) cells give rise to nematocysts, mucous glands, and sensory or nerve cells (2, 3). Many corals also precipitate calcium carbonate in the form of aragonite on a skeletal organic matrix (SOM) template (4, 5). The precipitation pattern is highly controlled between colonies, giving rise to morphological structures that are used as primary phenotypic markers of species in extant reefs and fossil samples.

The basic cellular processes responsible for the production of ECM, SOM, and calcium carbonate skeleton remain largely unknown. Molecular, genetic, and physiological analyses of cellular processes in corals have been elusive mainly because it is difficult to grow corals under controlled conditions in the laboratory and because of the genetic and physiological complexities inherent in associations of the animals with symbionts and parasites. All zooxanthellate corals harbor intracellular symbiotic dinoflagellates (zooxanthellae) within their endoderm cells; the algae provide up to 100% of the organic carbon and a significant fraction of the nitrogen requirements of the host (6). Corals also have symbiotic, parasitic, and mutualistic relation-

ships with a wide variety of prokaryotes and viruses (7), all of which greatly complicates molecular and genetic studies of cellular processes in the metazoan host. Establishing an *in vitro* coral cell culture could potentially circumvent these complications and also serve as a model for studying physiological processes at a cellular level. However, no continuous coral cell lines have been developed to date, and maintenance of primary cell cultures has encountered problems such as short-term viability or contamination by unicellular eukaryotic organisms, which eventually overgrow the original coral cells (8–13). Here we report on the development of a culturing system that significantly facilitates studies of coral cell physiology. By using this system, we examined the production of ECM, SOM, and calcium carbonate particles, which are the fundamental components that form the structure of the coral colony in nature.

## Results and Discussion

**Cell Culture Characterization.** Extracellular production of organic matrices and calcium carbonate particles was examined in primary, nondividing cell cultures of the soft coral *Xenia elongata* and the stony coral *Montipora digitata*. Cell cultures were comprised of ≈95% epithelium-like ectoderm or endoderm cells (the latter with or without zooxanthellae) ranging in size from 5 to 20 μm in diameter (Fig. 1), ≈1% nematocysts, ≈1% amoebocytes and <1% sensory nerve cells [supporting information (SI) Fig. 5]. The identification of cells was based on typical morphology and fluorescence (3). The cnidarian origin of cells in culture was verified by using 18S universal eukaryotic primers, and blasting the PCR-derived sequences against the National Center for Biotechnology Information nucleotide database ([www.ncbi.nlm.nih.gov](http://www.ncbi.nlm.nih.gov)) (SI Fig. 6).

*M. digitata* cells were more granular, smaller, and less spherical than *X. elongata* cells (Fig. 1 *b* and *a*, respectively). The fraction of zooxanthellae/zooxanthellae-containing endoderm cells was always higher in the *X. elongata* cell cultures. However, after 2 weeks, chlorophyll fluorescence was virtually undetectable in both cell cultures. The suppression of chlorophyll fluorescence depended on the concentration of glucose in the medium; cells cultured at low glucose concentrations (0.1 mM glucose; Fig. 7) maintained high chlorophyll levels. These results suggest that glucose can suppress chlorophyll synthesis in zooxanthellae, possibly as a result of end-product inhibition (14–16). The viability of both *M. digitata* and *X. elongata* cell cultures remained >80% over a period of ≈22 days (day 22: *M. digitata*, 83 ± 3%;

Author contributions: Y.H., M.Y.G., and P.G.F. designed research; Y.H., F.N., R.M.S., M.L., and V.S. performed research; Y.H., R.M.S., and P.G.F. analyzed data; and Y.H. and P.G.F. wrote the paper.

The authors declare no conflict of interest.

¶To whom correspondence should be sent at the \* address. E-mail: [falko@marine.rutgers.edu](mailto:falko@marine.rutgers.edu).

This article contains supporting information online at [www.pnas.org/cgi/content/full/0710604105/DC1](http://www.pnas.org/cgi/content/full/0710604105/DC1).

© 2007 by The National Academy of Sciences of the USA

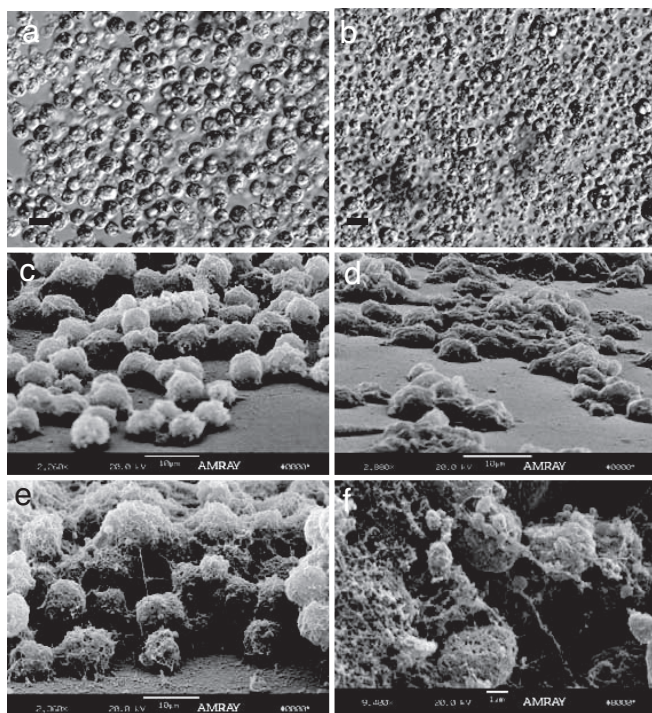


**Fig. 1.** Relief contrast and SEM images of coral cell cultures. (a and b) Relief contrast of *X. elongata* (a) and *M. digitata* (b). (c and d) SEM images showing the different types of ECM monolayer of adherent cells from *X. elongata* (c) and *M. digitata* (d). (e and f) multilayer adherent cell aggregates from *X. elongata* (e) and nonadherent cell aggregates from *M. digitata* (f). [Scale bars, 10  $\mu\text{m}$  (a–e) and 1  $\mu\text{m}$  (f).]

*X. elongata*,  $87 \pm 2\%$ ), after which it started to decrease (day 26: *M. digitata*,  $70 \pm 7\%$ ; *X. elongata*,  $75 \pm 6\%$ ). After the first week, many of the epithelial cells formed aggregates that adhered to the plates. Adhesion was best achieved on Primaria culture plates, which are coated with protonated amine groups and thus assume a positive charge. Because animal cells are characterized by a negative surface charge (17, 18), the initial attachment of cells to the plates presumably was attributable to electrostatic interactions.

**ECM Production.** The attached cells excreted ECM that mediated cell–cell as well as cell–substratum (plate surface) adhesion (Fig. 1 c–f). The ECM of both invertebrates and vertebrates is composed mainly of collagens, proteoglycans, and adhesive glycoproteins. The collagens (the fibrous structural proteins) are embedded in gels formed of polysaccharides (19, 20). SEM images of *M. digitata* and *X. elongata* cell aggregates indicate that the ECM formed *in vitro* indeed contained gel-like and fibrillar matrices (Fig. 1 c–f)

To examine the macromolecular composition of the ECM, we stained the cell cultures with Sirius red for collagen (21) and FITC–lectin conjugates of Con A and wheat germ agglutinin (WGA) for mannose/glucose and glucosamine/sialic acid residues in polysaccharides, respectively (22). These two classes of polysaccharides comprise the gel-like matrix in the ECM of *Pisaster ochraceus* (phylum, Echinodermata) (22) and were shown to comprise the heteropolysaccharide in collagen from the sea anemone *Metridium dianthus* (23). Sirius red, as well as Con A and WGA lectins, positively stained the ECM of both coral cell cultures (SI Fig. 8). Quantitative analysis (21) revealed that collagen accounted for  $7.1 \pm 0.7\%$  of the total cell protein in *X. elongata* cell cultures and  $6.2 \pm 0.5\%$  of that in *M. digitata*

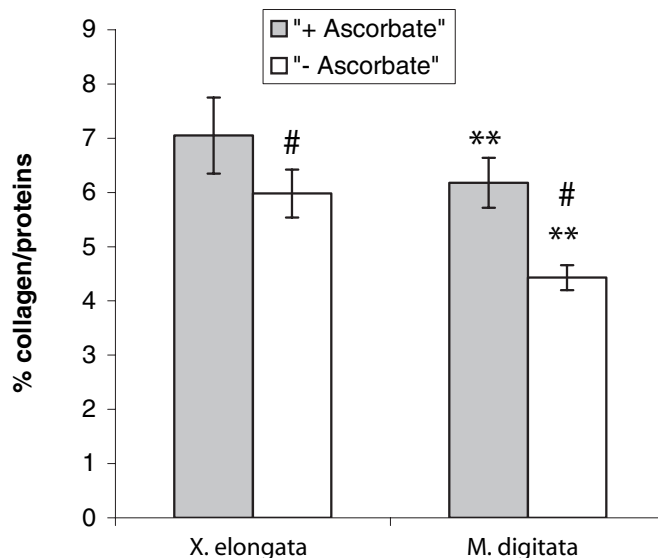


**Fig. 2.** Comparison between the percentage of collagen per total protein of *M. digitata* and *X. elongata* cell cultures in the absence or presence of ascorbic acid. The values are means  $\pm$  SEM ( $n = 5$ ). \*\*,  $P \leq 0.01$ ; #,  $P \leq 0.05$ .

(Fig. 2). Although WGA (SI Fig. 8) and Con A (data not shown) positively stained ECM and coral cell membranes, fluorometric quantification of polysaccharides in the ECM was not technically feasible.

Collagen is composed mainly of repeating glycine tripeptides with the sequence Gly-X-Y, where Y is frequently hydroxyproline (24). The hydroxylation of proline involves the activation of a reactive iron–oxygen complex, and ascorbic acid is required for the reduction of  $\text{Fe}^{3+}$  formed in this reaction (25). Previous studies have shown that the addition of ascorbic acid stimulates collagen production in many metazoans (26–32); however, its effect on collagen production in basal metazoans such as corals is not known. The addition of ascorbic acid to the culture media increased collagen production by  $\approx 40\%$  in *M. digitata* cell cultures ( $4.4 \pm 0.2$  weight percent collagen relative to total protein without ascorbic acid compared with  $6.2 \pm 0.5\%$  with ascorbic acid;  $P \leq 0.01$ ; Fig. 2); however, it had no significant effect on collagen production in *X. elongata* cell cultures ( $6.0 \pm 0.4\%$  without ascorbic acid and  $7.1 \pm 0.7\%$  with ascorbic acid;  $P \geq 0.05$ ). These results suggest either that collagen production in *X. elongata* cell cultures, in contrast to *M. digitata*, is independent of ascorbate (33) or that ascorbate is not a limiting substrate for the formation of hydroxyproline. Indeed, when cells were cultured in the absence of ascorbic acid, the fraction of ECM–collagen of *X. elongata* was significantly higher than that of *M. digitata* cell cultures ( $P \leq 0.05$ ; Fig. 2).

**Calcium Carbonate Precipitation.** After  $\approx 2$  weeks in culture, calcium carbonate-like particles, ranging in size from 20 to 100  $\mu\text{m}$ , were visible in *M. digitata* cell cultures (Fig. 3 and SI Fig. 9). Particles were observed within both adherent and nonadherent cell aggregates. The coverage of the particles by cells was not uniform and differed among the different aggregates (Fig. 3 and SI Fig. 9). Small mineral granules were also occasionally observed within *X. elongata* cell aggregates; however, these granules, which were spherical in shape and ranged in size from 10 to 20  $\mu\text{m}$ , were a relatively rare component and therefore were not analyzed further. The particles observed in *M. digitata* cell cultures were identified as calcium carbonate based on the dominance of the Ca signal over other elements. High-resolution inductively coupled plasma mass spectrometry confirmed these

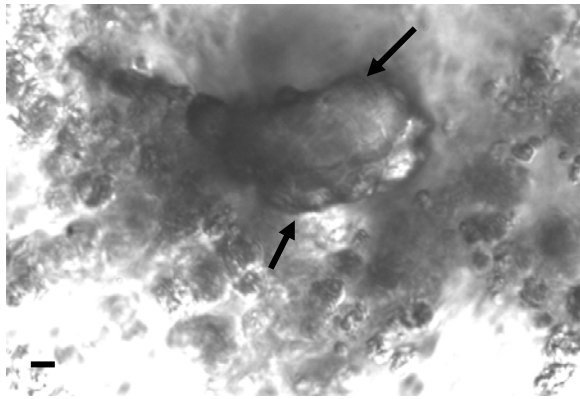


**Fig. 3.** Relief contrast microscope images of a 16-day-old *M. digitata* cell aggregate. The arrows indicate calcium carbonate particle. (Scale bar, 20  $\mu\text{m}$ .)

particles were aragonite based on Sr/Ca ratios ( $7.83 \text{ mmol mol}^{-1}$ ;  $n = 10$ ). Although this value is somewhat lower than that found in natural aragonitic coral skeletons ( $\approx 9.0$  to  $9.5 \text{ mmol mol}^{-1}$ ) (34), it is much higher than that of biogenic calcite (e.g.,  $1.15$  to  $1.45 \text{ mmol mol}^{-1}$  for foraminifera) (35). We therefore conclude that the particles associated with the cell aggregates were a low-Sr form of aragonite.

To confirm that the aragonite was formed *de novo*, we measured incorporation of  $^{45}\text{Ca}$  into acid labile macromolecules. The calcification rates in *M. digitata* cell cultures were approximately an order of magnitude higher than those in *X. elongata* [ $1.8 \pm 0.4$  and  $0.2 \pm 0.08 \text{ nmol of Ca per milligram of protein per hour}$ , respectively (mean  $\pm$  SEM;  $P \leq 0.001$ )].

**Skeletal Organic Matrix.** Studies of coral biomineralization indicate that calcification is mediated by the synthesis of an organic framework that induces nucleation and crystal growth (4, 5, 36, 37). Analyses of the organic materials extracted from coral skeletons show a composition of acidic amino acids (mainly glutamic and aspartic acid) and sulfated polysaccharides (5, 38–41). To examine whether such an organic matrix exists within the calcium carbonate particles produced *in vitro*, cell aggregates were suspended in HCl for mineral digestion. Fig. 4 *a–c* shows a time series of particle dissolution by HCl, revealing a mucus-like organic matrix within the particles. Alcian blue is commonly used to detect mucopolysaccharides and glycoproteins (42) and was shown to stain sulfated polysaccharides and protein compounds extracted from coral skeletons (5). Staining the organic matrix within the particles with Alcian blue at pH 2.5 verified the polysaccharidic nature of the organic substance (Fig. 4*d*).

Despite progress in the field of coral biomineralization, information regarding the synthesis of the SOM and the pathway of calcification is still scarce. By examining the effect of various culture media on the composition of the SOM, we can better understand the processes affecting this pathway. Furthermore, although precipitation of aragonite is an extracellular process, the complexity of the coral skeleton prevents easy access to the interface compartments where calcification occurs, making *in vivo* studies of this process difficult. However, the relatively simple structure of the cell aggregates overcomes this problem by providing easy access to the extracellular location.

*In vitro* aragonite crystallization has been described previously in coral cell cultures of *Pocillopora damicornis* (11). However, ECM and SOM production was not reported, and it was later shown that *P. damicornis* exhibits an 80% decrease in cell viability after 7 days in culture (12). Dispersed single cells also failed to reaggregate or attach to the culture surface, suggesting that cell adhesion mechanisms were inactive (12). The medium

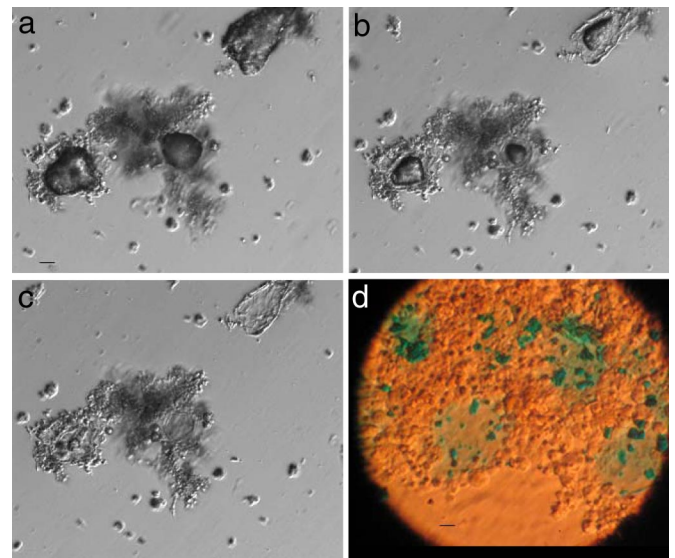


**Fig. 4.** Light microscope images of *M. digitata* cell cultures. (*a–c*) Time series showing acid dissolution of calcium carbonate particle within cell aggregates revealing the presence of an organic template: time 0 (*a*) and 30 s (*b*) and 60 s (*c*) after the addition of 0.6 M HCl. (Scale bar, 50  $\mu\text{m}$ .) (*d*) Twenty-day-old *M. digitata* adherent cell aggregates after HCl digestion and Alcian blue staining. The blue areas indicate the presence of mucopolysaccharides and glycoproteins. (Scale bar, 20  $\mu\text{m}$ .)

used in this study is unique in that it is supplemented with aspartic and glutamic acids, which are major components of the coral SOM (40). Glutamine was supplemented as GlutaMAX (Invitrogen) a glutamine dipeptide that does not break down into ammonium, which can be toxic to cells (43). Furthermore, the constant addition of ascorbic acid to the culture medium may also aid in maintaining high cell viability because of its role as an antioxidant (44), as well as its importance for collagen production (24).

The results presented in this report reveal that coral cells maintain the ability to precipitate calcium carbonate on an ECM *in vitro*, while further excreting a matrix for cell–cell and cell–substratum organization. These processes are similar to bone formation and ECM production in higher metazoans. For example, both calcium carbonate precipitation in coral skeleton and calcium phosphate precipitation in bone result from mineral crystallization deposited on an organic matrix scaffold (45, 46). In addition, the SOM of both vertebrates and corals is composed mainly of acidic amino acids and polysaccharides (45, 46). The compatibility of coral skeleton as human implants (47, 48) further demonstrates the similarity between bone formation and coral calcification. Moreover, the ECM composition of corals is similar to that of higher metazoans (both in invertebrates as well as vertebrates) (19, 20, 49) and its production is considered to be a fundamental process in the evolution of multicellularity in animals (50). The cell culture system described here allows for detailed understanding of cellular processes that control calcification and ECM production in this basal metazoan group; the evolution of such processes were key events in the early evolution of metazoans.

## Materials and Methods

**Corals.** Two coral species were used in this study: the soft coral *X. elongata* and the stony coral *M. digitata*. Each species originated from one parent colony that was collected from reefs off of western Australia (Ashmore reef) and has been growing in an 800-liter, custom-designed aquarium as described previously (51).

**Cell Cultures.** To initiate cell cultures, small fragments of coral were excised from parent colonies and incubated for 2.5 h, with gentle shaking, in calcium-free artificial seawater supplemented with 3% antibiotics–antimycotics solution (GIBCO), prepared as described previously (12). The medium was replaced with artificial seawater 34‰ (Instant Ocean sea salt, Aquarium Systems) and 25 mM HEPES supplemented with collagenase (Sigma) at a final concentration of 1.5 mg/ml, and fragments were incubated for an additional 0.5 h. Fragments were then transferred to 35 × 10 mm Primaria culture dishes (two fragments in each dish; VWR International, Inc.). The plates contained 3 ml of the following culture medium: artificial seawater 34‰ (Instant Ocean sea salt, Aquarium Systems), 25 mM HEPES pH = 8.0, 2% heat-inactivated FBS (Invitrogen), MEM vitamin solution 50×, MEM amino acid mix 100× (Sigma), GlutaMAX 2 mM (Invitrogen), aspartic acid 20 μg/ml, taurine 10 mM (Sigma), 1% antibiotic–antimycotics solution (GIBCO), 0.1–3 mM glucose, and 50 μg/ml L-ascorbic acid (added every other day). After 24 h, fragments were removed from the plates, and the medium with cells was passed (three times) through a custom-built sterile cell strainer. Cell strainers were made by cutting off a 15-ml falcon tube into 3.5-cm-long columns and attaching, by heat, a 20-μm nylon mesh on one side. This insured the removal of tissue debris from the medium. Cells were maintained in a humidified chamber on a 12/12 h light/dark cycle at 26°C. After 24 h, cell strainers containing the coral fragments were removed from the plates. The medium was replaced with fresh medium, initially after 5 days and then every 7 days.

**Microscopy Imaging.** Light and fluorescence microscopy imaging was carried out with an inverted IX71 epifluorescence microscope (Olympus) equipped with a QImaging Retiga EXi SVGA high-speed monochromatic cooled CCD camera system and IPLab for Mac (version 4.0.5) for image processing and analysis. For SEM of adherent cells, cells were fixed for 24 h with 2% formalin and gently washed with distilled water. After fixation, culture plates were cut into 1-cm<sup>2</sup> pieces, followed by dehydration with an ascending ethanol series (70–100%) and critical point drying by using liquid CO<sub>2</sub>. Samples were then coated with gold and platinum and observed on an AMRAY-1830I microscope (Amaray, Inc.).

**Cell Viability Measurements.** Cell viability was quantitatively assessed by using Sytox green. Cells were incubated with 50 μM Sytox green for 15 min in the dark and visualized with an inverted IX71 epifluorescence microscope (Olympus). A total of 100–200 cells from three different optical fields of two culture plates were counted for each measurement ( $n = 6$ ).

**DNA Extraction 18S rDNA Amplification and Sequencing.** For DNA extraction, cells were harvested and frozen in liquid nitrogen, followed by phenol/chloroform extraction and alcohol precipitation (52).

18S rDNA was amplified by PCR with general eukaryotic primers (5'-ACCTGGTTCCTGATCCAG-3', 5'-TGATCCTTCYGCAGGTTAC-3') as described previously (53). PCR products were purified with the minielute gel extraction kit (Qiagen) and were then cloned and transformed to TOP10 chemically competent bacteria by using the TOPO cloning kit (Invitrogen). Plasmids were purified by the QIAprep spin miniprep kit (Qiagen) and sequenced by using a 3100-Avant automatic sequencer (Applied Biosystems).

**Quantification of Collagen and Total ECM Proteins.** Collagen and proteins were quantified by colorimetric analyses by using Sirius red and Fast green as described previously (54). This method used the selective binding of Sirius red F3BA to collagen protein and Fast green FCF (Sigma) to noncollagen protein when both are dissolved in aqueous saturated picric acid. Briefly, culture plates were incubated with 1 ml of saturated picric acid solution that contained 0.1% Sirius red F3BA and 0.1% Fast green FCF. The plates were incubated at room temperature for 30 min in a rotary shaker. The fluids were

then carefully withdrawn, and the plates were washed repeatedly with distilled water until the fluid was colorless. After washing, 1 ml of 1:1 (vol/vol) 0.1% NaOH and absolute methanol was added to the plates to elute the color. The eluted color was immediately read by using a spectrophotometer at 540 and 605 nm.

**Lectin Staining.** Cells were fixed with 2% formalin (vol/vol) before labeling with FITC–lectin conjugates of Con A and WGA (Sigma). After washing with artificial sea water, culture plates were incubated with 100 μM either lectin for 1.5 h at in the dark. Plates were then washed twice to remove excess stain and were observed with an epifluorescence inverted microscope with FITC-suitable filters.

**High-Resolution Inductively Coupled Plasma Mass Spectrometry.** Precipitated mineral particles were pooled from three culture plates for inorganic analysis. The pooled cultures were incubated in 1 M NaOH at 90°C for 45 min to digest organic matter, then rinsed repeatedly with distilled water adjusted to pH 8 with NaOH. Particles were then rinsed with 0.065 M HNO<sub>3</sub>, the rinsing solution was removed by aspirating through a small pipette tip, and the particles were dissolved in 0.1 M HNO<sub>3</sub> with sonication for 1 h (particles visibly dissolved). A 100-μl aliquot of this solution was diluted with 300 μl of 0.5 M HNO<sub>3</sub> and analyzed for multiple elements, including Sr and Ca, by high-resolution inductively coupled plasma mass spectrometry against matrix-matched mixed-element standards (55).

**Calcification Measurements.** Calcification rates were measured as described in ref. 56 with modifications to adjust it for cell cultures (57). Briefly, cell cultures were incubated with 1 ml of culture medium containing 1 μCi of <sup>45</sup>Ca (as CaCl<sub>2</sub>, 22.13 mCi/ml; PerkinElmer) for 18 h. Cultures were maintained at 26°C under light (50 μmol of photons per meter squared per second) with gentle shaking (30 rpm). At the end of the incubation period, cells were scraped with a rubber policeman, and the medium containing calcium carbonate particles and cells was centrifuged at 20,000 × *g* for 2 min; the supernatant was retained for radioactive counting. Cells were washed until the supernatant did not contain radioisotope (five washes). Pellets were then resuspended in 0.5 ml of 1 M NaOH and incubated for 20 min at 90°C to dissolve organic tissue, followed by centrifugation at 20,000 × *g* for 20 min. (The supernatant was kept for protein determination.) The pellets were then washed with distilled water (pH 8) and resuspended with 0.5 ml of 6 M HCl for 18 h to dissolve the calcium carbonate particles. The samples were then added to 4.5 ml of scintillation liquid (Packard) and counted in a LS6000IC scintillation counter (Beckman).

Protein concentration was determined by using the BCA protein determination kit according to the protocol of the manufacturer (Pierce).

**Exposure of Skeletal Organic Matrix and Alcian Blue Staining.** Alcian blue solution was prepared in acetic acid 3% (10 g/liter). For decalcification, cultures were incubated in 1 M HCl until calcium carbonate particles had dissolved, followed by gentle washing with artificial seawater. Samples were then incubated with Alcian blue solution (pH 2.5) for 30 min, followed by washing with artificial seawater.

**Statistic Analysis.** Unless otherwise stated, all data were expressed as means ± SE. The Student's *t* test was used to compare the differences between groups. A two-sample equal variance test was used when comparing the same coral species before and after treatment. A two-sample unequal variance test was used when comparing between the hard and the soft coral. Probability values of <0.05 were considered significant.

**ACKNOWLEDGMENTS.** The research was supported by the Strategic Environmental Research and Development Program (P.G.F. and M.Y.G.), a Bikura Postdoctoral fellowship (Y.H.), and the Rutgers University Center for Marine Biotechnology.

1. Bridge D, Cunningham CW, Desalle R, Buss LW (1995) Class-level relationships in the phylum Cnidaria: Molecular and morphological evidence. *Mol Biol Evol* 12:679–689.
2. Peterson KJ, Eernisse DJ (2001) Animal phylogeny and the ancestry of bilaterians: Inferences from morphology and 18S rDNA gene sequences. *Evol Dev* 3:170–205.
3. Brusca RC, Brusca GJ (1990) Phylum Cnidaria in Invertebrates, ed Sinauer AD (Sinauer, Sunderland, MA), pp 211–262.
4. Allemand D, Tambutte E, Girard JP, Jaubert J (1998) Organic matrix synthesis in the scleractinian coral *Stylophora pistillata*: Role in biomineralization and potential target of the organotin tributyltin. *J Exp Biol* 201:2001–2009.
5. Cuif JP, Dauphin Y (2005) The environment recording unit in coral skeletons: A synthesis of structural and chemical evidences for a biochemically driven, stepping-growth process in fibres. *Biogeosciences* 2:61–73.
6. Falkowski PG, Dubinsky Z, Muscatine L, Porter J (1984) Light and the bioenergetics of a symbiotic coral. *Bioscience* 34:705–709.
7. Yokouchi H, et al. (2006) Whole-metagenome amplification of a microbial community associated with scleractinian coral by multiple displacement amplification by using phi 29 polymerase. *Environ Microbiol* 8:1155–1163.
8. Frank U, Rabinowitz C, Rinkevich B (1994) In vitro establishment of continuous cell cultures and cell lines from ten colonial cnidarians. *Mar Biol* 120:491–499.
9. Rinkevich B (1999) Cell cultures from marine invertebrates: Obstacles, new approaches and recent improvements. *J Biotechnol* 70:133–153.
10. Kopecky EJ, Ostrander GK (1999) Isolation and primary culture of viable multicellular endothelial isolates from hard corals. *In Vitro Cell Dev Biol Anim* 35:616–624.
11. Domart-Coulon IJ, et al. (2001) Aragonite crystallization in primary cell cultures of multicellular isolates from a hard coral, *Pocillopora damicornis*. *Proc Natl Acad Sci USA* 98:11885–11890.
12. Domart-Coulon IJ, Tambutte S, Tambutte E, Allemand D (2004) Short term viability of soft tissue detached from the skeleton of reef-building corals. *J Exp Mar Biol Ecol* 309:199–217.

13. Rinkevich B (2005) Marine invertebrate cell cultures: New millennium trends. *Mar Biotechnol* 7:429–439.
14. Beale SI, Appleman D (1971) Chlorophyll synthesis in *Chlorella* regulation by degree of light limitation of growth. *Plant Physiol* 47:230–235.
15. Lewitus AJ, Kana TM (1994) Responses of estuarine phytoplankton to exogenous glucose: Stimulation versus inhibition of photosynthesis and respiration. *Limnol Oceanogr* 39:182–189.
16. Radchenko IG, Il'yash LV, Fedorov VD (2004) Effect of exogenous glucose on photosynthesis in the diatom *Thalassiosira weissflogii* depending on nitrate nitrogen supply and illumination. *Biol Bull* 31:67–74.
17. Yamamoto K, Yamamoto M, Ooka H (1988) Changes in negative surface charge of human diploid fibroblasts, TIG-1, during in vitro aging. *Mech Ageing Dev* 42:183–195.
18. Raz I, Havivi Y, Yarom R (1988) Reduced negative surface charge on arterial endothelium of diabetic rats. *Diabetologia* 31:618–620.
19. Har-el R, Tanzer ML (1993) Extracellular matrix 3: Evolution of the extracellular matrix in invertebrates. *FASEB J* 7:1115–1123.
20. Czaker R (2000) Extracellular matrix (ECM) components in a very primitive multicellular animal, the dicyemid mesozoan *Kantharella antarctica*. *Anat Rec* 259:52–59.
21. Esteban FJ, et al. (2005) Colorimetric quantification and in situ detection of collagen. *J Biol Educ* 39:183–186.
22. Reimer CL, Crawford BJ, Crawford TJ (1992) Basement membrane lectin binding sites are decreased in the esophageal endoderm during the arrival of presumptive muscle mesenchyme in the developing asteroid *Pisaster ochraceus*. *J Morphol* 212:1887–1995.
23. Katzman RL, Kang AH (1972) The presence of fucose, mannose, and glucosamine-containing heteropolysaccharide in collagen from the sea anemone *Metridium dianthus*. *J Biol Chem* 247:5486–5489.
24. Peterkofsky B, Udenfriend S (1965) Enzymatic hydroxylation of proline in microsomal polypeptide leading to formation of collagen. *Proc Natl Acad Sci USA* 53:335–342.
25. Peterkofsky B (1991) Ascorbate requirement for hydroxylation and secretion of procollagen: relationship to inhibition of collagen synthesis in scurvy. *Am J Clin Nutr* 54:1135–1140.
26. Murad S, et al. (1981) Regulation of collagen synthesis by ascorbic acid. *Proc Natl Acad Sci USA* 78:2879–2882.
27. Chojkier M, Houglum SK, Solis-Herruzog J, Brenner DA (1989) Stimulation of collagen gene expression by ascorbic acid in cultured human fibroblasts. A role for lipid peroxidation? *J Biol Chem* 264:16957–16962.
28. Darr D, Combs S, Pinnell S (1993) Ascorbic-acid and collagen-synthesis: Rethinking a role for lipid-peroxidation. *Arch Biochem Biophys* 307:331–335.
29. Franceschi RT, Iyer BS, Cui YQ (1994) Effects of ascorbic-acid on collagen matrix formation and osteoblast differentiation in murine MC3T3-E1 cells. *J Bone Miner Res* 9:843–854.
30. Torii Y, Hitomi K, Tsukagoshi N (1994) L-Ascorbic-acid 2-phosphate promotes osteoblastic differentiation of MC3T3-E1 mediated by accumulation of type-I collagen. *J Nutr Sci Vitaminol* 40:229–238.
31. Phillips CL, Combs SB, Pinnell SR (1994) Effects of ascorbic-acid on proliferation and collagen-synthesis in relation to the donor age of human dermal fibroblasts. *J Invest Dermatol* 103:228–232.
32. Tsuneto M, Yamazaki H, Yoshino M, Yamada T, Hayashi S (2005) Ascorbic acid promotes osteoclastogenesis from embryonic stem cells. *Biochem Biophys Res Commun* 335:1239–1246.
33. Parsons KK, et al. (2006) Ascorbic acid-independent synthesis of collagen in mice. *Am J Physiol Endocrinol Metab* 290:E1131–E1139.
34. Linsley BK, Wellington GM, Schrag DP (2000) Decadal sea surface temperature variability in the subtropical South Pacific from 1726 to 1997 AD. *Science* 290:1145–1148.
35. Elderfield H, Vautravers M, Cooper M (2002) The relationship between shell size and Mg/Ca, Sr/Ca, delta O-18, and delta C-13 of species of planktonic foraminifera. *Geochim Geophys Geosys* 3:1–13.
36. Goldberg WM (2001) Acid polysaccharides in the skeletal matrix and calciblastic epithelium of the stony coral *Mycetophyllia reesi*. *Tissue Cell* 33:376–387.
37. Muscatine L, et al. (2005) Stable isotopes (delta C-13 and delta N-15) of organic matrix from coral skeleton. *Proc Natl Acad Sci USA* 102:1525–1530.
38. Cuif JP, Dauphin Y, Gautret P (1999) Compositional diversity of soluble mineralizing matrices in some recent coral skeletons compared to fine-scale growth structures of fibres: discussion of consequences for biomineralization and diagenesis. *Int J Earth Sci* 88:582–592.
39. Gautret P, Cuif JP, Stolarski J (2000) Organic components of the skeleton of scleractinian corals: Evidence from in situ acridine orange staining. *Acta Palaeontol Pol* 45:107–118.
40. Puverel S, et al. (2005) Soluble organic matrix of two Scleractinian corals: Partial and comparative analysis. *Comp Biochem Physiol B Biochem Mol Biol* 141:480–487.
41. Dauphin Y, Cuif JP, Massard P (2006) Persistent organic components in heated coral aragonitic skeletons—Implications for palaeoenvironmental reconstructions. *Chem Geol* 231:26–37.
42. Spicer SS, Baron DA, Sato A, Schulte BA (1981) Variability of cell surface glycoconjugates: Relation to differences in cell function. *J Histochem Cytochem* 29:994–1002.
43. Hassell T, Gleave S, Butler M (1991) Growth inhibition in animal cell culture. The effect of lactate and ammonia. *Appl Biochem Biotechnol* 30:29–41.
44. Meister A (1992) On the antioxidant effects of ascorbic acid and glutathione. *Biochem Pharmacol* 44:1905–1915.
45. Gorski JP (1992) Acidic phosphoproteins from bone matrix: A structural rationalization of their role in biomineralization. *Calcif Tissue Int* 50:391–396.
46. Clode PL, Marshall AT (2003) Calcium associated with a fibrillar organic matrix in the scleractinian coral *Galaxea fascicularis*. *Protoplasma* 220:153–161.
47. Lynch CC, et al. (2005) The murine coral implant model of bone metastasis. *J Bone Miner Res* 20:P34–P35.
48. Gao TJ, et al. (1997) The use of a coral composite implant containing bone morphogenetic protein to repair a segmental tibial defect in sheep. *Int Orthop* 21:194–200.
49. Young SD (1975) Collagen in the autoclave-soluble proteins of scleractinian corals (Cnidaria). *Comp Biochem Physiol B* 50:105–107.
50. Morris PJ (1993) The developmental role of the extracellular matrix suggests a monophyletic origin of the kingdom Animalia. *Evolution (Lawrence, Kans)* 47:152–165.
51. Tchernov D, et al. (2004) Membrane lipids of symbiotic algae are diagnostic of sensitivity to thermal bleaching in corals. *Proc Natl Acad Sci USA* 101:13531–13535.
52. Sambrook J, Fritsch EF, Maniatis T (1989) *Molecular Cloning: A Laboratory Manual* (Cold Spring Harbor Lab Press, Cold Spring Harbor, NY).
53. Moon-van der Staay SY, et al. (2000) Abundance and diversity of prymnesiophytes in the picoplankton community from the equatorial Pacific Ocean inferred from 18S rDNA sequences. *Limnol Oceanogr* 45:98–109.
54. Leon AL-D, Rojkind M (1985) A simple micromethod for collagen and total protein determination in formalin-fixed paraffin-embedded sections. *J Histochem Cytochem* 33:737–743.
55. Rosenthal Y, Field MP, Sherrell RM (1999) Precise determination of element/calcium ratios in calcareous samples using sector field inductively coupled plasma mass spectrometry. *Anal Chem* 71:3248–3253.
56. Tambutte E, et al. (1995) An improved Ca-45 protocol for investigating physiological mechanisms in coral calcification. *Mar Biol* 122:453–459.
57. Wu SY, et al. (2003) Endothelin-1 is a potent regulator in vivo in vascular calcification and in vitro in calcification of vascular smooth muscle cells. *Peptides* 24:1149–1156.